













In-Depth Metallurgical and Microstructural Analysis of Oneshape and Heat Treated Onecurve Instruments

 Arash AZIZI,  Carlo PRATI,  Riccardo SCHIAVON,  Raquel FITZGIBBON,  Chiara PIRANI,  Francesco IACONO,  Gian Andrea PELLICIONI,  Andrea SPINELLI,  Fausto ZAMPARINI,  Pietro PUDDU,  Giovanni BOLELLI,  Luigi GENERALI

ABSTRACT

Objective: To define surface, mechanical, microstructural and metallurgical features of conventional OneShape (OShape) and heat-treated OneCurve (OCurve) nickel-titanium instruments.

Methods: Instruments were analysed by scanning electron microscopy (SEM) on new instruments and after simulated clinical use (SCU). Cyclic fatigue testing was performed and the number of cycles to fracture (NCF) and the length of the fractured instruments were measured (Mann-Whitney test). Fractured instruments during cyclic fatigue testing were then inspected by SEM fractographic analysis. Field emission gun scanning electron microscopy (FEG-SEM), energy-dispersive X-ray spectroscopy (EDX) and micro-Raman spectroscopy were used to assess alloy surface chemistry. Focused ion beam (FIB) was performed to analyse the oxide layer on the surface of OCurve before and after SCU. X-Ray diffraction (XRD), metallographic evaluation and differential scanning calorimetry (DSC) were used to determine martensitic/austenitic phase transformation temperatures.

Results: SEM observations on new instruments revealed a smooth regular surface with flattened milling grooves. No wear features were detected after SCU. OCurve exhibited a higher cyclic fatigue resistance ($P < 0.05$), slower crack propagation and a surface layer of TiO_2 . Metallographic analysis and XRD showed the prevalence of martensitic grains on OCurve instruments that were stable at body temperature as confirmed by DSC analysis. Furthermore, DSC demonstrated a shift in the temperature transformation ranges suggesting an increase of martensite phase in autoclaved OCurve instruments.

Conclusion: Heat treatment processes were confirmed as a valid enhancement of the properties of the new generation NiTi instruments. OCurve presented a significant improvement over OShape regarding both mechanical and metallurgical characteristics.

Keywords: Differential scanning calorimetry, martensitic instruments, OneCurve, OneShape, wear analysis, X-Rays spectrometry

Please cite this article as: Azizi A, Prati C, Schiavon R, Fitzgibbon R, Pirani C, Iacono F, Pelliccioni GA, Spinelli A, Zamparini F, Puddu P, Bolelli G, Generali L. In-Depth Metallurgical and Microstructural Analysis of Oneshape and Heat Treated Onecurve Instruments. *Eur Endod J* 2021; 6: 90-7

From the Department of Biomedical and Neuromotor Sciences DIBINEM (A.A. ✉ arash.azizi@studio.unibo.it, C.P., R.S., R.F., C.P., F.I., G.A.P., A.S., F.Z.) Endodontic Clinical Section, Faculty of Dentistry, University of Bologna, Bologna, Italy; Department of Engineering Enzo Ferrari (DIEF) (P.P., G.B.), University of Modena and Reggio Emilia, Modena, Italy; Department of Surgery (L.G.), Medicine, Dentistry and Morphological Sciences with Transplant Surgery, Oncology and Regenerative Medicine Relevance (CHIMOMO), University of Modena and Reggio Emilia, Modena, Italy

Received 08 September 2020,
Accepted 11 January 2021

Published online: 23 March 2021
DOI 10.14744/eej.2021.63634

This work is licensed under a Creative Commons Attribution-NonCommercial 4.0 International License.



HIGHLIGHTS

- OCurve presented a significant improvement over OShape regarding mechanical and metallurgical characteristics.
- OCurve instruments showed a higher fatigue resistance after autoclave sterilisation, likely attributed to a shift in temperature transformation and an increase of martensite phase.
- Post manufacturing processes were confirmed as a valid enhancement of the mechanical properties of new generation NiTi instruments.

INTRODUCTION

Despite wide range of nickel-titanium (NiTi) mechanical instruments, they still present disadvantages such as insufficient instrument flexibility, unexpected instrument separation (1) and poor debris removal from root canals (2). Instrument separation is caused by torsional fatigue, cyclic fatigue, or most commonly a combination of both, representing a major concern for clinicians as removal is not always possible (3).

The NiTi manufacturing industry has strived to reduce these unwanted complications. In recent years, alloy heat treatments have been promising. Through the utilisation of heat treatment, the martensite/austenite transformation temperatures have been shifted, permitting a higher concentration of martensitic phase

during clinical instrumentation and a predictable treatment due to superior mechanical properties (4).

Instrument sequence simplification has been proposed through single-file systems as canal preparation may be faster than that obtainable with conventional multi-file sequences (5).

OneShape (OShape) (MicroMega, Besançon, France) instruments appeared in the dental market in 2011 as the first single-file shaping system conceived for continuous rotation movement. Made of a conventional austenite 55-NiTi alloy, the design consists of a size 25/.06 file with a passive tip and a variable cross-section (5). This variable design involves a triangular cross-section with three sharp cutting edges in the apical and middle portions, which progressively changes to two cutting edges near the shaft. Furthermore, the instrument is intended for single-patient usage, in order to avoid cross-contamination.

OneCurve (OCurve) (MicroMega, Besançon, France) endodontic instruments were recently commercialised as the improved version of OShape instruments. These instruments, maintaining the same design of their precursors OShape and have been treated with a patented heat process (C.Wire) to grant an improved flexibility and an enhanced shape memory that renders the instrument pre-bendable (6).

The aim of this research was to evaluate the mechanical, microstructural and metallurgical features of both instruments, in order to better understand the properties and the improvements have been obtained with the new manufacturing procedures.

MATERIALS AND METHODS

The results of the analysis included in this study are presented in Table 1.

SEM analysis and wear test after simulated clinical use (SCU)

Four new OCurve and 4 OShape were evaluated under scanning electron microscopy (SEM) (JSM-5200, JEOL, Tokyo, Japan) at increasing magnification from 50× to 5000×. Micrographs were acquired at the tip of the instrument and on cutting edges at 5 mm from the tip to detect overall superficial morphology. Ethics committee approval (Prot. n. 0067265-05.06.2019 of CE-AVEC) and informed consent were obtained.

To detect wear features by SEM, each instrument was tested in human extracted teeth for simulated clinical use (SCU). Each instrument was used in 4 straight canals of extracted teeth which were identified through two-dimensional radiographs that evaluated the mesiodistal and buccolingual canal curvatures (7, 8). Crowns were removed with a water-cooled diamond wheel saw in order to obtain standard root lengths of 15 mm. Canal patency was verified with manual #10 and 15 K-file (Dentsply Maillefer, Baillagues, Switzerland) and working length was determined by insertion of a 25 mm #10 K file until its tip appeared at the apical foramen. Flaring of the coronal third of the root canal was achieved with OneFlare 25/0.09 L17 mm (MicroMega, Besançon, France) and glide-path with OneG 14/0.09 L25 mm (MicroMega, Besançon, France). OCurve and OShape instruments were used with a 16:1 reduction hand-

piece (X-Smart Plus, Dentsply Maillefer, Baillagues, Switzerland) following manufacturer's directions, at 350 rpm and 2.5 N-cm, with pecking motion. Irrigation was performed with 3 ml of 5% NaOCl (Nicolor 5, Ognà, Muggiò, Italy) and 3 ml of 10% EDTA (Tubuliclean, Ognà, Muggiò, Italy).

After SCU, each instrument was washed in an ultrasonic bath for 10 min and then autoclaved at 134.8 °C. Micrographs were taken by SEM at the same points and angulations of the first examination to identify surface alterations index for wear features such as presence of unwinding, microcracks, blade disruption and tip deformation (9-11).

Cyclic fatigue testing (CFT) and SEM fractographic analysis

CFT was performed to evaluate the time and number of cycles to fracture (NCF) of new OCurve 25/.06 (n=20) and OShape 25/.06 (n=20) instruments. The instruments were tested in stainless steel AISI 300 block containing a simulated canal with an angle of curvature of 90°, a radius of 5 mm and the center of the curvature at 7 mm from the tip of the file. A handpiece was mounted and fixed on a mobile apparatus, which approached or separated from a second platform, providing a precise and standardised placement of each file inside the artificial canal. A slipping Plexiglas top face cover allowed visualisation of the instruments rotating in the canal until fracture occurred. Time to fracture was visually recorded with a digital stopwatch (3M ESPE, St. Paul, MN, USA).

Additional OCurve instruments (n=10) were subjected to the same CFT after 1 cycle of autoclave sterilisation (OCurve AS) at 134.8°C to detect the effect of sterilisation procedures on this instruments.

The NCF was calculated by the following formula: $NCF = \text{Time (s)} \times \text{rotating speed (rpm)} \times 60 \text{ s}^{-1}$ (12, 13) and the length of fractured fragments was measured using a digital caliper (14).

Field emission gun scanning electron microscopy (FEG-SEM - Nova NanoSEM 450, FEI, Eindhoven, Netherlands) was used to observe the fractographic features of fractured instruments in an axial view and micrographs at 200× to 3000× were taken (15). Everhart-Thornley Detector and Through-the-lens were used as detectors. In order to obtain a clear surface, samples were polished in an ultrasonic bath containing a solution of methyl ethyl ketone, alcohol, H₂O and isopropyl alcohol for 15 min immediately before placing in the FEG-SEM.

EDX analysis

Two new OCurve and 2 OShape instruments were subjected to energy-dispersive X-ray spectroscopy (EDX) (QUANTAX-200, Bruker, Billerica, Massachusetts, USA) by an unbiased operator in randomly selected areas of the working portion of the instruments, in order to assess the overall chemical composition of the NiTi surface.

Micro-Raman spectroscopy

OCurve and OShape surface was analysed with micro-Raman spectroscopy to complete data on chemical surface composition, provided by EDX. An optical microscope (Olympus BX40, Olympus Global, Tokyo, Japan) equipped with micro-Raman (LabRAM, Horiba - Jobin Yvon, Kyoto, Japan) was used. Spectra were acquired using a He:Ne $\lambda=532.05$ nm green monochro-

matic light (laser) source. Long focal distance 50 to 100× objectives were employed to focus the laser beam on the surface of the samples in the working part and near the shaft. New and after SCU of both instruments were analysed.

Focused Ion beam (FIB) analysis

FIB analysis was used to study the surface of oxide layers on new and after SCU of an OCurve instrument (n=1). The instrument was analysed by in-situ sectioning inside a dual-beam machine (Strata™ DB235, FEI), equipped with a high-resolution FIB column having a gallium ion source and a FEG-SEM column. Sections were made on a relatively flat region along the working part of the instruments. Briefly, a protective platinum layer was first deposited on the area of interest by ion beam-assisted chemical vapor deposition using a metal-organic precursor. The cross-section was then milled by FIB using high beam current (7 nA), up to a depth of ≈5 μm, and its side wall was polished using lower beam current (300 pA) to remove any possible ion beam-induced damage from the milling stage. The cross-section was finally observed under a tilt angle of 52° using the FEG-SEM column (16, 17).

X-Ray diffraction analysis (XRD)

XRD was done to evaluate the inner composition of internal phases. New and after SCU instruments of OShape (n=2) and OCurve (n=2) were sectioned in 2 transversal portions. These sections were embedded at a room temperature setting epoxy resin and ground under constant water flow with progressively finer abrasive papers (#P320 to #P2500 grit size) until complete exposure of the axial cross section of the NiTi instruments. Final polishing was obtained with a polycrystalline diamond paste (3 μm) and a silica paste (50 nm). XRD (XRD-X'Pert Pro, PANALytical, Almelo, Netherlands) was performed in order to provide data concerning crystallographic features and phase composition of the instruments. XRD was performed at room temperature (≈25°C) with Cu-Kα monochromatic radiation generated by an X-ray tube set at 40 kV and 40 mA. The range for the acquisition was 30°<2θ<100° with a step size of 0.017° and acquisition time of 1100 s/step, using a 1D-array of solid state detectors (X'Celerator, PANALytical). XRD patterns were analysed using the X'Pert Highscore Plus software for phase identification (PANALytical) (18, 19).

Metallographic analysis

Metallographic analysis was performed on new and after SCU OCurve (n=2) and OShape (n=2) to visualise crystallographic features of the inner part of the NiTi instruments. Each instrument was sectioned and embedded at a room temperature in epoxy resin, ground and polished as described for XRD. Chemical etching was performed with a solution consisting of 60% nitric acid, 30% acetic acid and 10% hydrofluoric acid for 10 seconds in order to disclose the metallographic features (20). Optical microscope analysis (Leica DMI 5000M, Wetzlar, Germany) focused at the tip of the instruments, at 5 mm from the tip and near the handle. Micrographs between 50× and 1000× were taken.

Differential scanning calorimetry

To assess the phase transformation temperatures, differential scanning calorimetry (DSC-Q2000, TA Instrument, New Castle, DE, USA) was performed. The working part of new and after

SCU OCurve (n=1) and OShape (n=1) was sectioned in 3 parts and a mass between 5 and 15 mg was placed in a melting pot.

The NiTi parts inside the melting pot were subjected to 2 heating and 2 cooling thermal cycles with heat flow variation set at 5°C min⁻¹ within a temperature range between -40°C and 110°C [18, 19] starting from 20°C. Plots were analysed using Universal Analysis 2000 (TA Instrument) software to obtain onset temperatures of phase transformations and enthalpy changes (ΔH). Transformation temperatures were obtained from the intersection between extrapolation of the baseline and maximum gradient line of the lambda-type DSC curve (21, 22).

Statistical analysis

Time to fracture, NCF and length of fractured fragments measured from the cyclic fatigue test were analysed by Mann-Whitney test. The level of significance was set at P<0.05.

RESULTS

Results of analyses are summarized in Table 1.

SEM and wear test after SCU

No surface alterations were observed on new instruments. Interestingly, after SCU and sterilisation procedures no microcracks, unwinding, blade disruption or tip deformation were noticed. Presence of dentine debris was noticed on the surface of all instruments after SCU (Fig. 1). Both OShape and OCurve new instruments revealed the presence of many round grooves in the interface between the shaft and the first spire portion. Grooves were measured using the corresponding FEG-SEM tool and measurements ranged between 3.93 μm and 28.26 μm (Fig. 2).

CFT and SEM fractographic analysis

OCurve instruments exhibited a significantly higher time to fracture (88.81±13.03 sec vs 13.50±7.74 sec) and NCF compared to OShape (P<0.05) (Table 2). No statistically significant differences were found between the groups for length of fractured instruments. Additional OCurve instruments tested after 1 cycle of autoclave sterilisation demonstrated a significantly higher NCF compared to non-autoclaved OCurve instruments (P<0.05). Fractographic analysis revealed the presence of propagation of fatigue striations corresponding to the initiation of the superficial crack. OCurve instruments showed the propagation of the fatigue striations corresponding to the initiation of the crack. A wide dimpled area was noticeable in the upper side of micrograph. In OS, the fractographic surface was totally covered by dimples (Fig. 3).

EDX

EDX confirmed that both OShape and OCurve samples consisted of nearly equiatomic NiTi alloys. Both OCurve and OShape surface exhibited nickel, titanium and oxygen. OCurve showed an oxygen peak more evident than OShape.

Micro-Raman spectroscopy

No discernible Raman signal was produced by the working surface of the OShape samples, both new instruments and after SCU. The working surface of OCurve samples, by contrast, produced a discernible Raman signal, characterized by peaks at 250 cm⁻¹, 430 cm⁻¹ and 600 cm⁻¹. This spectrum can be as-

TABLE 1. Results of the analysis carried out during evaluation of OShape and Ocurve instruments

Tools	n	Analysis	After SCU	Evaluation criteria	Results
SEM	4 OCurve 4 OShape	Wear test	Yes	- Overall morphology - Microcracks - Fractures - Unwindings - Blade disruption - Debris - Tip deformation	No evidence of wear was noticed; debris still present after sterilization protocol
Cyclic fatigue testing machine	20 OCurve 20 OShape 10 OCurve AS	CFT	No	- Time until fracture (T) - NCF	T and NCF of OCurve were significantly higher than OShape OCurve AS showed even a higher T and NCF than OCurve and OShape
FEG-SEM	2 OCurve 2 OShape	Fractographic analysis	No	- Crack initiation points - Striation areas - Dimples - Ductile fracture area	Multiple initiation points and wide striation areas in OCurve; single initiation points and little striation areas in OShape
EDX	2 OCurve 2 OShape	Surface chemical analysis	Yes	- Chemical composition of surface	Both OCurve and OShape surface exhibited Ni, Ti and O; O peak was more evident in OCurve than OShape
Raman	1 OCurve 1 OShape	Surface chemical analysis	Yes	- Chemical composition of surface	Presence of TiO ₂ (rutile) on OCurve surface
XRD	3 OCurve 3 OShape	Inner cristallographic composition	Yes	- Martensite - Austenite - R-phase	At 25°C the main composition of both OCurve and OShape is austenitic; OCurve showed presence of martensite and R-phase
Metallographic microscope	2 OCurve 2 OShape	Inner cristallographic composition	Yes	- Martensite - Austenite - R-phase - Grain distribution	OCurve showed more presence of martensite grains compared to OShape
DSC	1 OCurve 1 OShape	Inner cristallographic composition	Yes	- Temperatures of phase transformation	OCurve is mainly martensitic at body temperature; OShape is austenitic
FIB	1 OCurve	Surface oxide layer measure	Yes	- Oxide layer thickness	A thin (<100nm) oxide layer was observed in OCurve; the layer was too thin to be determined

SCU: Simulated clinical use, CFT: Cyclic fatigue test, NCF: Number of cycles to fracture, OCurve: OneCurve, OShape: OneShape, OCurve AS: OCurve after one cycle of autoclave sterilization

cribed to titanium oxide (TiO₂) in its rutile polymorph. In both instruments, shafts were covered by a thick rutile layer that produced a distinct Raman spectrum (23).

Focused ion beam (FIB) analysis

A surface layer was observed on new OCurve instruments, which remained present after SCU. The thickness was too low (<100 nm) to be quantified, even when imaged with a high-resolution FEG-SEM column.

XRD

At room temperature (approximately 25°C), austenite was the main constituent of both OCurve and OShape instruments. OShape instruments contained minor amounts of martensite,

TABLE 2. Cyclic fatigue test results. Mean, standard deviations (SD) and P value of the Time to failure (sec), Number of cycles to fracture (NCF) and the length of the fractured fragment of the tested instruments

	Time to failure (sec±SD)	NCF (mean±SD)	Fracture length (mm±SD)
OShape	13.50±7.74 ^a	74.30±45.72 ^a	7.41±0.47 ^a
OCurve	88.81±13.03 ^b	517.35±76.20 ^b	7.34±1.33 ^a
OCurve AS	110.10±22.42 ^c	642.06±130.80 ^c	7.14±0.86 ^a

P value set at 0.05. Superscript letters indicate statistical differences between groups. NCF: Number of cycles to fracture, OCurve: One curve, OCurve AS: One curve after 1 cycle of autoclave sterilization, OShape: One shape

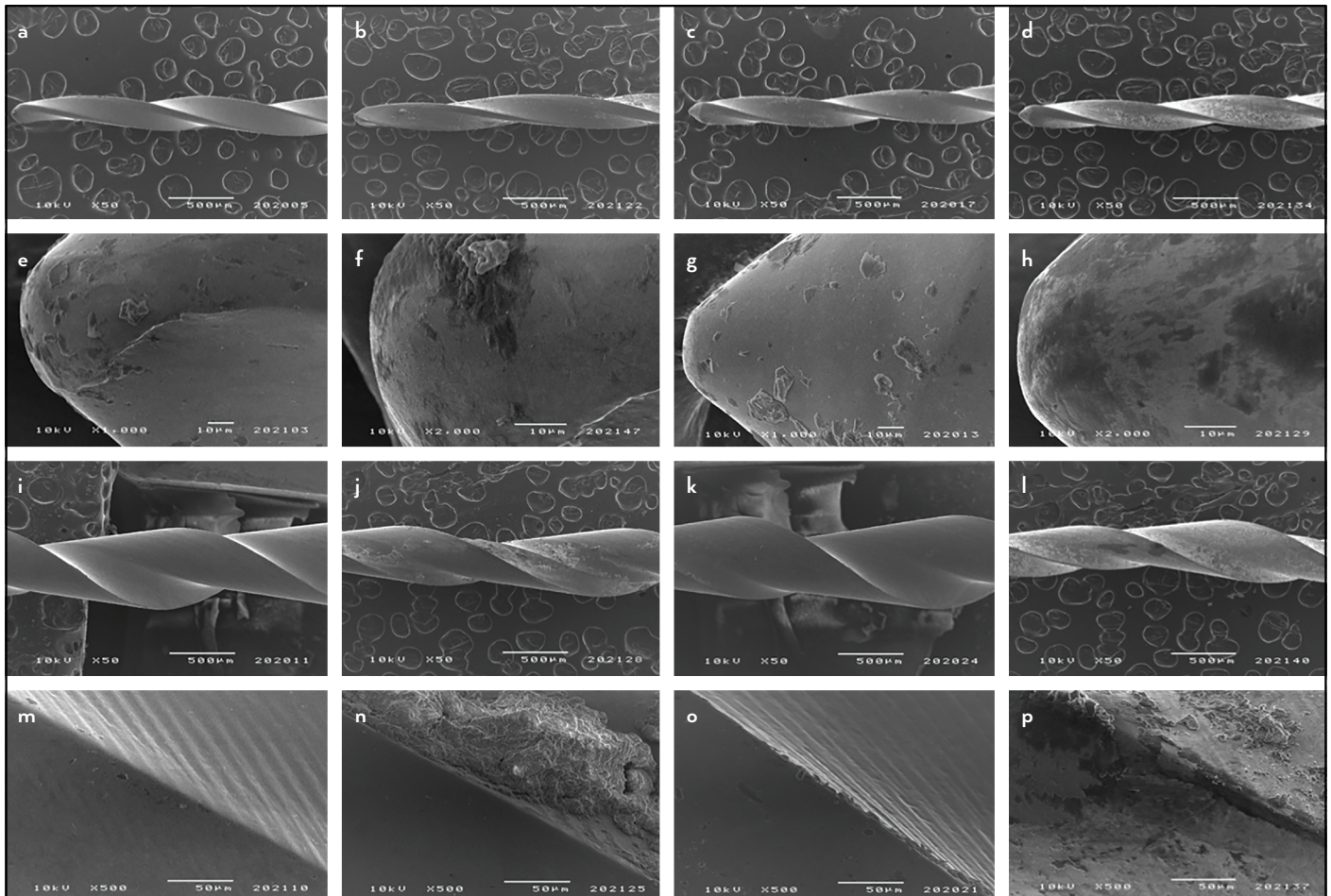


Figure 1. Micrographs of O Shape (a, b, e, f, i, j, m, n) and O Curve (c, d, g, h, k, l, o, p) instruments before and after simulated clinical use (SCU) at the same points and angulations. Tip (a-h) and cutting edges at 5 mm from the tip (i-p) were inspected at increasing magnification (50x–5000x) to verify wear features. Round grooves were detected on new instruments (a, c, e, g, i, k, m, o) and debris were noticeable on the surface of used instruments (b, d, f, h, j, l, n, p)

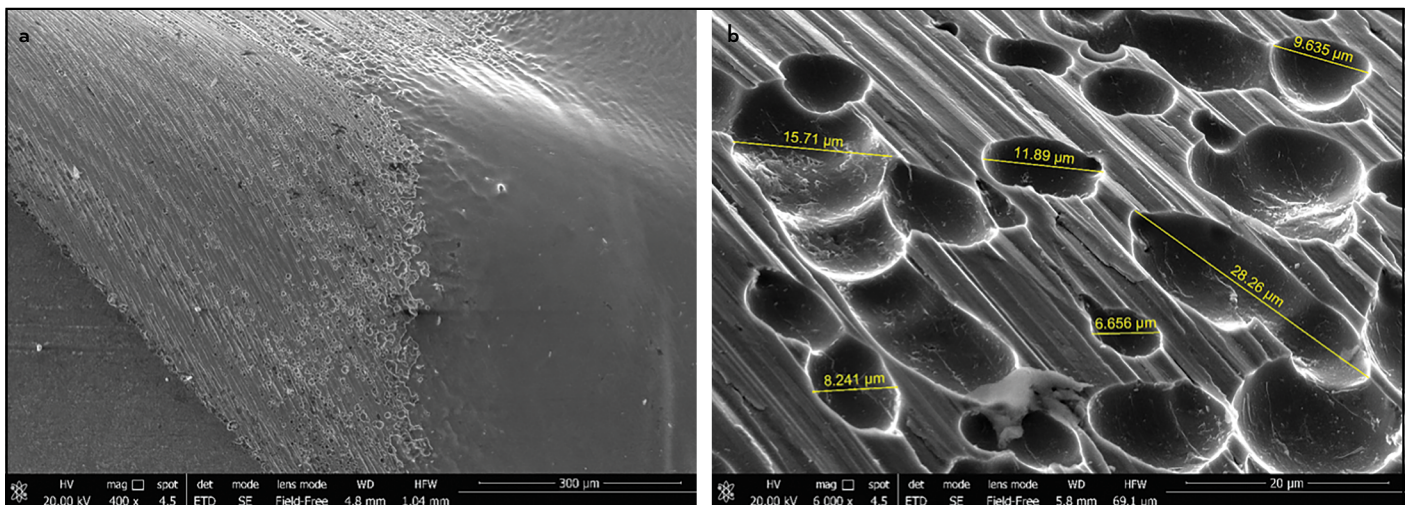


Figure 2. SEM micrographs of OCurve instruments revealing the presence of grooves (range 3.93 µm–28.26 µm) on the surface of the shaft at lower (400x) and higher (6000x) magnification

whereas both martensite and R-phase were detected as minor phases in OCurve instruments.

After SCU and autoclave sterilisation, OShape instruments showed no changes. On the contrary, OCurve instruments

presented a significantly increased R-phase amount. The main diffraction peak at $2\theta \approx 42^\circ$ was split into two distinct components which were austenite and R-phase. A substantial amount of the latter had therefore appeared together with austenite.

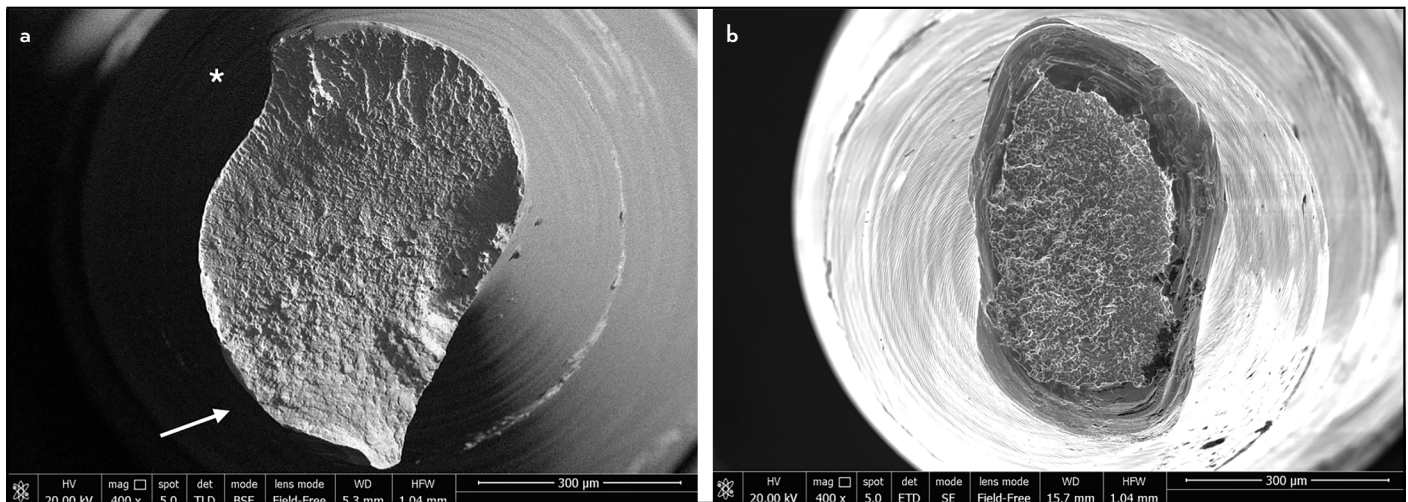


Figure 3. Fractographic analysis of OCurve (a) and OShape (b) instruments showed the propagation of the fatigue striations (white arrow) in correspondence of the initiation of the crack. A wide dimpled area is noticeable (*) in the upper side of micrograph. In OShape (b), the fractographic surface was totally covered by dimples

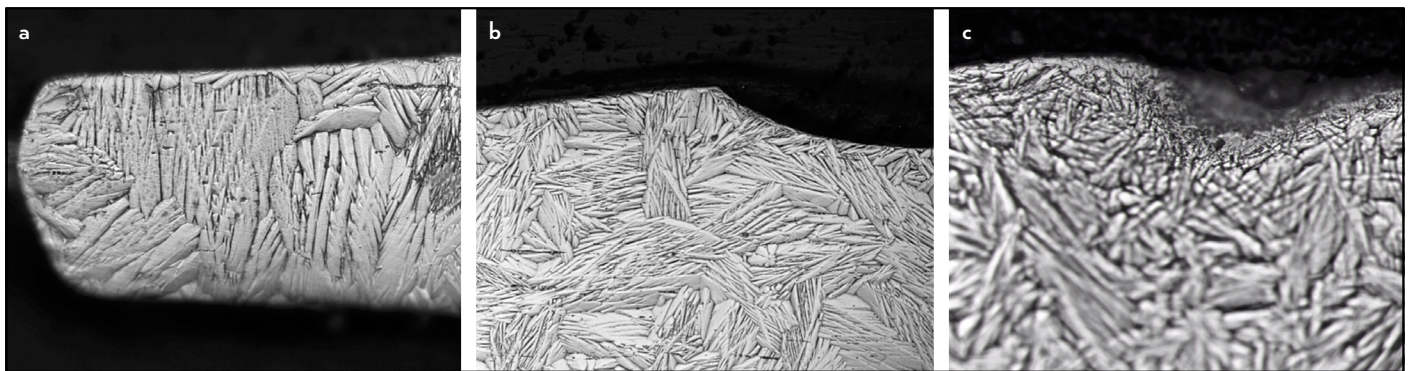


Figure 4. Metallurgical analysis of OCurve instrument: tip (a) and coronal portion (b) of new file; coronal portion of SCU file (c). Prevalence of martensitic grains with parallel orientation in correspondence of the tip and randomly oriented in the coronal portion on the OCurve instruments was disclosed

Metallographic analysis

OCurve instruments exhibited a superior percentage of martensite in analysed sections that were characterized by the presence of many small acicular grains compared to OShape (Fig. 4). The martensitic grains were mostly randomly oriented in the coronal portion and had parallel orientation in correspondence of the tip portion of instrument.

On the contrary, OShape instruments showed mainly an austenitic phase, characterised by diffuse large and flat grains.

Differential scanning calorimetry (DSC)

OShape instruments exhibited a single, broad DSC peak during both heating and cooling stages (Fig. 5a). The peak extends over a temperature range of approximately 10°C (M_s –martensitic start) to -28°C (M_f –martensitic finish) during cooling (forward transformation), whereas it shifts to slightly higher values, namely between -15°C (A_s –austenitic start) to 19°C (A_f –austenitic finish), during heating (reverse transformation).

OCurve instruments had a remarkably different behavior (Fig. 5b). The DSC peak is sharper, with higher overall transformation enthalpy of 4.7 to 4.9 J/g. The temperature range was approximately from 46°C (M_s) to 3°C (M_f) during cooling (for-

ward transformation), from 10°C (A_s) to 49°C (A_f) during heating (reverse transformation).

In both instruments, SCU did not appreciably modify enthalpy values and transformation temperature ranges.

DISCUSSION

OCurve and OShape instruments share the exact file design and differ exclusively on the NiTi alloy heat treatment. Both OShape and OCurve instruments are subjected to a post-manufacturing electropolishing treatment. This induces the removal of most imperfections and inconsistencies due to the manufacturing process in order to improve the superficial features (24). The round groves between the shaft and the first spire observed in new instruments during SEM analysis are presumed to be a consequence of this treatment (Fig. 2).

Neither OCurve nor OShape instruments exhibited microcracks, tip deformations, fractures, unwindings, blade disruptions after SCU use. Therefore, it can be assumed that both presented adequate wear resistance to the SCU protocol, which is close to the clinical condition where NiTi instruments operate.

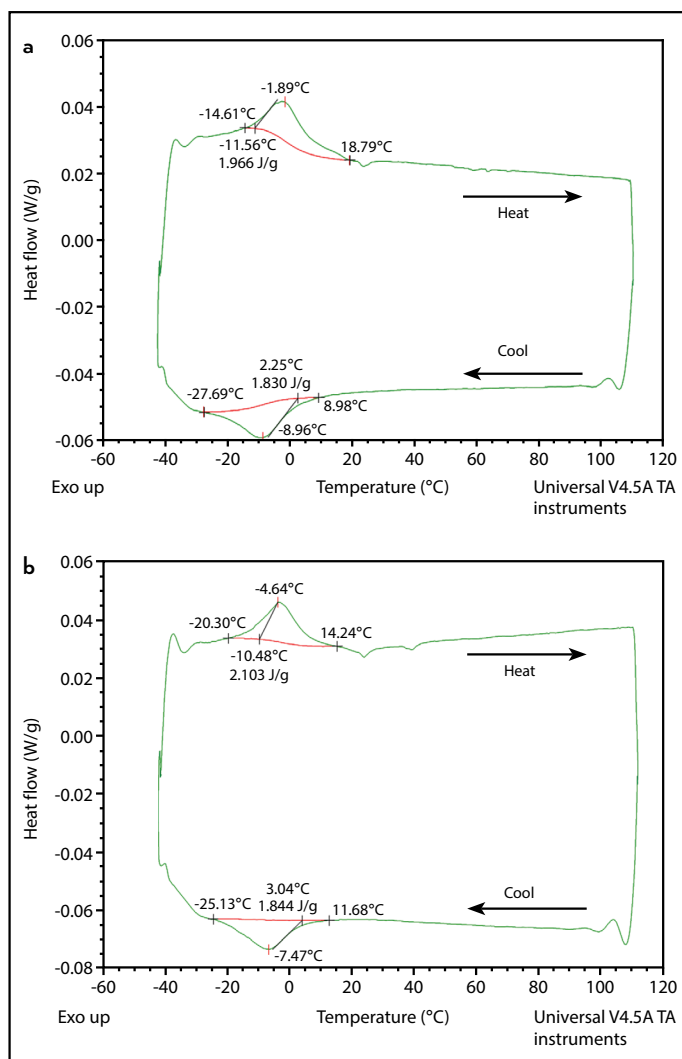


Figure 5. DSC traces of new and SCU OShape instruments (a) and OCurve instruments (b)

Time to fracture and NCF values were almost 7 times superior in OCurve compared to OShape instruments, suggesting the heat treatment performed on OCurve allows a safer clinical use in multirooted teeth or in complex anatomy. Fractographic analysis of OCurve revealed a wider area covered by fatigue striations than in OShape, thus suggesting a slower fracture propagation after surface microcrack origin and, therefore, a higher resistance. This data further confirms the mechanical properties improvement of OCurve when compared to OShape instruments.

A macroscopically visible yellow golden layer was observable on the surface of the working portion of OCurve, a new feature that was not present on OShape. To ascertain the nature of this layer, Raman and EDX spectra were performed, demonstrating the presence of a thin but perceivable layer of TiO₂, in its thermodynamically more stable rutile polymorph, on the surface of OCurve instruments. This layer, as seen in FIB-machined sections can be observed only on OCurve samples and not on OShape samples. It is known (25) that TiO₂ films presenting an around or below 100 nm thickness produce interference colours which can fall within the yellow-orange spectrum as

was found concerning OCurve. Therefore, we can assume that this layer might be caused by heat treatment. Even though the treatment was likely performed under vacuum or inert atmosphere, a very low oxygen partial pressure would have been enough to cause slight surface oxidation of the alloy, due to Ti-O high affinity. For instance, an Ellingham diagram for the standard free energy of formation of metal oxides shows that, at 800°C, the oxidation of Ti becomes thermodynamically spontaneous at as low an oxygen partial pressure as 10-34 atm.

Raman and FIB analyses indeed showed that the TiO₂ film was still present after SCU. Therefore, we can assume that no significant amount of metal debris was released from the instrument surface during its usage, even if it was not possible to determine whether any thickness change occurred after SCU due to the TiO₂ film thickness below 100 nm.

The post-production heat-treatment resulted in clear differences between the two instruments in terms of phase composition and phase transformation behavior, which can be comprehended by combining XRD and DSC results: OShape instruments consist primarily of austenite at the XRD acquisition temperature of ≈25°C. The broad DSC peak (Fig. 5a) is typical of an austenite ↔ martensite transition, and austenite conversion into martensite during cooling occurs at ≈10°C in both new and SCU instruments. It is therefore inferred that OShape instruments also consist of austenite at the human body temperature (≈37°C), because martensite formation during cooling only starts at Ms≈10°C, as DSC revealed. Instruments used after SCU were also primarily austenitic after a high-temperature sterilisation in autoclave. The small amount of martensite detected in XRD patterns might consist of a stable, non-transformable phase, which cannot be removed by austenisation during the autoclave treatment. This is also corroborated by the rather low transformation enthalpy of OShape instruments (<3 J/g): a complete austenite → martensite transformation would indeed be characterised by greater enthalpy. An analogous occurrence of non-transformable martensite has recently been noted in another NiTi endodontic instrument (26).

By contrast, OCurve instruments are in a multi-phase condition at the XRD acquisition temperature of ≈25°C. This is fully consistent with transformation ranges in the DSC curves (Fig. 5b). The latter also indicates that the multi-phase structure is maintained up to the actual operative temperature (≈37°C). The transformation range during both heating and cooling, indeed, extends to >40°C in new OCurve instruments, and shifts to even higher values after SCU. This observation means that heating in an autoclave affects the eventual phase composition of OCurve instruments at body temperature. As confirmed in CFT on new OCurve instruments after 1 cycle of autoclave sterilization, the increase of the martensite transformation point can condition mechanical properties such as cyclic fatigue resistance. The sharp DSC peak is consistent with the formation of R-phase, accordingly detected in XRD patterns. A two-stage transition from austenite to R-phase and finally to martensite was therefore inferred. The increased amount of R-phase in the XRD pattern of SCU OCurve instruments, acquired after cooling from the autoclave sterilisation tempera-

ture, was perfectly consistent with a forward transformation peak located at ≈ 29 to 30°C (DSC curves in Fig. 5b). Indeed, it means that, after full austenisation in the autoclave, cooling to room temperature leaves the OCurve instruments fully within its forward transformation range.

Taking into account the limitations of this study, we can affirm that thermal treatments of OCurve instruments modify the intrinsic chemical and mechanical characteristics, providing reasons for a safer clinical use in root canal shaping.

CONCLUSION

OC instruments presented a significant improvement over the previous OShape version, in terms of NFC, time to fracture and a different morphology of fracture surface. Within the limitations of this study, OCurve appears a promising and safer root canal shaping instrument. Post manufacturing processes were confirmed as a valid enhancement of the mechanical properties of new generation NiTi instruments.

Disclosures

Conflict of interest: All authors declare that they have no conflict of interest.

Ethics Committee Approval: This study was approved by Comitato Etico Indipendente di Area Vasta Emilia Centro Ethics Committee. (Prot. n. 0067265-05.06.2019 of CE-AVEC)

Peer-review: Externally peer-reviewed.

Financial Disclosure: The author(s) received no funding for this work.

Authorship contributions: Concept – A.A., ; Design – C.Prati, C.Pirani, A.S.; Supervision – R.S., G.A.P., F.Z.; Funding – F.I., A.S., P.P., L.G.; Materials – R.S., P.P., G.B., L.G.; Data collection &/or processing – R.S., P.P., G.B., L.G.; Analysis and/or interpretation – R.F., F.I., G.A.P., A.S., G.B.; Literature search – C.Prati, G.A.P., L.G.; Writing – A.A., C.Prati, R.F., C.Pirani, F.Z., L.G.; Critical Review – A.A., C.Prati, R.F., F.Z., L.G.

REFERENCES

- Peters OA. Current challenges and concepts in the preparation of root canal systems: a review. *J Endod* 2004; 30(8):559–67. [\[CrossRef\]](#)
- Prati C, Foschi F, Nucci C, Montebugnoli L, Marchionni S. Appearance of the root canal walls after preparation with NiTi rotary instruments: a comparative SEM investigation. *Clin Oral Investig* 2004; 8(2):102–10.
- Parashos P, Messer HH. Rotary NiTi instrument fracture and its consequences. *J Endod* 2006; 32(11):1031–43. [\[CrossRef\]](#)
- Zupanc J, Vahdat-Pajouh N, Schäfer E. New thermomechanically treated NiTi alloys - a review. *Int Endod J* 2018; 51(10):1088–103. [\[CrossRef\]](#)
- Bürklein S, Benten S, Schäfer E. Shaping ability of different single-file systems in severely curved root canals of extracted teeth. *Int Endod J* 2013; 46(6):590–7. [\[CrossRef\]](#)
- Ertuğrul İF. Effect of sodium hypochlorite on the cyclic fatigue resistance: A scanning electron microscopy evaluation. *Microsc Res Tech* 2019; 82(12):2089–94. [\[CrossRef\]](#)
- Kosti E, Zinelis S, Molyvdas I, Lambrianidis T. Effect of root canal curvature on the failure incidence of ProFile rotary Ni-Ti endodontic instruments. *Int Endod J* 2011; 44(10):917–25. [\[CrossRef\]](#)
- Pirani C, Cirulli PP, Chersoni S, Miele L, Ruggeri O, Prati C. Cyclic fatigue testing and metallographic analysis of nickel-titanium rotary instruments. *J Endod* 2011; 37(7):1013–6. [\[CrossRef\]](#)
- Troian CH, S6 MV, Figueiredo JA, Oliveira EP. Deformation and fracture of RaCe and K3 endodontic instruments according to the number of uses. *Int Endod J* 2006; 39(8):616–25. [\[CrossRef\]](#)
- Pirani C, Paolucci A, Ruggeri O, Bossù M, Polimeni A, Gatto MR, et al. Wear and metallographic analysis of WaveOne and reciproc NiTi instruments before and after three uses in root canals. *Scanning* 2014; 36(5):517–25.
- Caballero H, Rivera F, Salas H. Scanning electron microscopy of superficial defects in Twisted files and Reciproc nickel-titanium files after use in extracted molars. *Int Endod J* 2015; 48(3):229–35. [\[CrossRef\]](#)
- Iacono F, Pirani C, Arias A, de la Macorra JC, Generali L, Gandolfi MG, et al. Impact of a modified motion on the fatigue life of NiTi reciprocating instruments: a Weibull analysis. *Clin Oral Investig* 2019; 23(7):3095–102.
- Pirani C, Iacono F, Generali L, Sassatelli P, Nucci C, Lusvarghi L, et al. HyFlex EDM: superficial features, metallurgical analysis and fatigue resistance of innovative electro discharge machined NiTi rotary instruments. *Int Endod J* 2016; 49(5):483–93. [\[CrossRef\]](#)
- Topçuoğlu HS, Topçuoğlu G, Kafdağ Ö, Arslan H. Cyclic fatigue resistance of new reciprocating glide path files in 45- and 60-degree curved canals. *Int Endod J* 2018; 51(9):1053–8. [\[CrossRef\]](#)
- Shen Y, Huang X, Wang Z, Wei X, Haapasalo M. Low environmental temperature influences the fatigue resistance of nickel-titanium files. *J Endod* 2018; 44(4):626–9. [\[CrossRef\]](#)
- Bolelli G, Sabiruddin K, Lusvarghi L, Gualtieri E, Valeri S, Bandyopadhyay PP. FIB assisted study of plasma sprayed splat–substrate interfaces: NiAl–stainless steel and alumina–NiAl combinations. *Surf Coat Technol* 2010; 205(2):363–71. [\[CrossRef\]](#)
- Generali L, Borghi A, Lusvarghi L, Bolelli G, Veronesi P, Vecchi A, et al. Evaluation of the usage-induced degradation of Genius and Reciproc nickel-titanium reciprocating instruments. *Odontology* 2019; 107(4):473–81. [\[CrossRef\]](#)
- Iacono F, Pirani C, Generali L, Bolelli G, Sassatelli P, Lusvarghi L, et al. Structural analysis of HyFlex EDM instruments. *Int Endod J* 2017; 50(3):303–13. [\[CrossRef\]](#)
- Generali L, Puddu P, Borghi A, Brancolini S, Lusvarghi L, Bolelli G, et al. Mechanical properties and metallurgical features of new and ex vivo used Reciproc Blue and Reciproc. *Int Endod J* 2020; 53(2):250–64. [\[CrossRef\]](#)
- Pirani C, Ruggeri O, Cirulli PP, Pelliccioni GA, Gandolfi MG, Prati C. Metallurgical analysis and fatigue resistance of WaveOne and ProTaper nickel-titanium instruments. *Odontology* 2014; 102(2):211–6. [\[CrossRef\]](#)
- Yahata Y, Yoneyama T, Hayashi Y, Ebihara A, Doi H, Hanawa T, et al. Effect of heat treatment on transformation temperatures and bending properties of nickel-titanium endodontic instruments. *Int Endod J* 2009; 42(7):621–6. [\[CrossRef\]](#)
- Hou X, Yahata Y, Hayashi Y, Ebihara A, Hanawa T, Suda H. Phase transformation behaviour and bending property of twisted nickel-titanium endodontic instruments. *Int Endod J* 2011; 44(3):253–8. [\[CrossRef\]](#)
- Lafuente B, Downs RT, Yang H, Stone N. The power of databases: the RRUFF project. In: Armbruster T, Danisi RM, editors. *Highlights in Mineralogical Crystallography*. Berlin, Germany: W. De Gruyter; 2015. p. 1–30.
- Praisantti C, Chang JW, Cheung GS. Electropolishing enhances the resistance of nickel-titanium rotary files to corrosion-fatigue failure in hypochlorite. *J Endod* 2010; 36(8):1354–7. [\[CrossRef\]](#)
- Diamanti MV, Del Curto B, Pedferri MP. Interference colors of thin oxide layers on titanium. *Color Res Appl* 2008; 33(3):221–8. [\[CrossRef\]](#)
- Jouliia A, Bolelli G, Gualtieri E, Lusvarghi L, Valeri S, Vardelle M, et al. Comparing the deposition mechanisms in suspension plasma spray (SPS) and solution precursor plasma spray (SPPS) deposition of yttria-stabilised zirconia (YSZ). *J Eur Ceram Soc* 2014; 34(15):3925–40. [\[CrossRef\]](#)